Journal Pre-proof

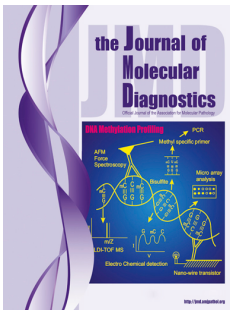

Design of a comprehensive fluorescence *in situ* hybridization assay for genetic classification of T-cell acute lymphoblastic leukemia

Roberta La Starza, Valentina Pierini, Tiziana Pierini, Valeria Nofrini, Caterina Matteucci, Silvia Arniani, Martina Moretti, Anair G. Lema Fernandez, Fabrizia Pellanera, Danika Di Giacomo, Tiziana C. Storlazzi, Antonella Vitale, Paolo Gorello, Gabriella Sammarelli, Giovanni Roti, Giuseppe Basso, Sabina Chiaretti, Robin Foà, Claire Schwab, Christine J. Harrison, Pieter Van Vlierberghe, Cristina Mecucci

PII: S1525-1578(20)30043-X

DOI: https://doi.org/10.1016/j.jmoldx.2020.02.004

Reference: JMDI 896

To appear in: *The Journal of Molecular Diagnostics*

Received Date: 6 August 2019

Revised Date: 29 January 2020

Accepted Date: 3 February 2020

Please cite this article as: La Starza R, Pierini V, Pierini T, Nofrini V, Matteucci C, Arniani S, Moretti M, Lema Fernandez AG, Pellanera F, Di Giacomo D, Storlazzi TC, Vitale A, Gorello P, Sammarelli G, Roti G, Basso G, Chiaretti S, Foà R, Schwab C, Harrison CJ, Van Vlierberghe P, Mecucci C, Design of a comprehensive fluorescence *in situ* hybridization assay for genetic classification of T-cell acute lymphoblastic leukemia, *The Journal of Molecular Diagnostics* (2020), doi: https://doi.org/10.1016/j.jmoldx.2020.02.004.

Design of a comprehensive fluorescence *in situ* hybridization assay for genetic classification of T-cell acute lymphoblastic leukemia

Roberta La Starza,[1] Valentina Pierini,[1] Tiziana Pierini,[1] Valeria Nofrini,[1] Caterina Matteucci,[1] Silvia Arniani,[1] Martina Moretti,[1] Anair G Lema Fernandez,[1] Fabrizia Pellanera,[1] Danika Di Giacomo,[1] Tiziana C Storlazzi,[2] Antonella Vitale,[3] Paolo Gorello,[1] Gabriella Sammarelli,[4] Giovanni Roti,[4] Giuseppe Basso,[5] Sabina Chiaretti,[3] Robin Foà,[3] Claire Schwab,[6] Christine J Harrison,[6] Pieter Van Vlierberghe,[7] Cristina Mecucci[1]

Footnote: R.L.S. and V.P. contributed equally to this work.

[1]Hematology and Bone Marrow Transplantation Unit, Department of Medicine, Molecular Medicine Laboratory, University of Perugia, Italy

[2]Department of Biology, University of Bari "Aldo Moro", Italy

[3]Hematology, Department of Translational and Precision Medicine, Sapienza University, Rome, Italy

[4]Hematology and Bone Marrow Transplantation Unit, Department of Medicine and Surgery, University of Parma, Italy

[5]Pediatric Hemato-Oncology, Department of Pediatrics “Salus Pueri”, University of Padova, Italy

[6]Leukaemia Research Cytogenetic Group, Northern Institute for Cancer Research, Newcastle University, Newcastle-upon-Tyne, UK

[7]Department of Biomolecular Medicine, Ghent University, Belgium

Short running title: Molecular-cytogenetic diagnosis in T-ALL

Funding: Supported by AIRC (Grant number: IG-15525), PRIN 2017 (code 2017PPS2X4), Sergio Luciani Association, Fabriano, and Fondazione Cassa di Risparmio Perugia (Grant numbers: 2016.0113.021 to C.M. and 2018.0418.021 to R.L.S.). T.P. was supported by a grant from SIES 2018 (A. Maiolo specializzata in citogenetica). P.V.V. was supported by the European Research Council (ERC starting grant 639784). C.S. was supported by Bloodwise, UK; G.R by an AIRC Start-up Investigator Grant (n. 17107 G.R.)

Disclosures: None declared.

Corresponding authors:

Cristina Mecucci, Hematology and Bone Marrow Transplantation Unit, Department of Medicine, Molecular Medicine Laboratory, CREO, P.le Menghini 9, 06132 Perugia, Italy. Phone: ++39 0755783808; Fax ++39 0755783691 cristina.mecucci@unipg.it

Roberta La Starza, Hematology and Bone Marrow Transplantation Unit, Department of Medicine, Molecular Medicine Laboratory, CREO, P.le Menghini 9, 06132 Perugia, Italy. Phone: ++39 0755783455; Fax ++39 0755783691 roberta.lastarza@unipg.it

Abstract

T-cell acute lymphoblastic leukemia (T-ALL) results from deregulation of a number of genes via multiple genomic mechanisms. We designed a comprehensive fluorescence *in situ* hybridization assay (CI-FISH) which consists of genomic probes to simultaneously investigate oncogenes and oncosuppressors recurrently involved in chromosome rearrangements in T-ALL which was applied to 338 T-ALL cases. CI-FISH provided genetic classification into one of the well-defined genetic subgroups, ie, *TAL/LMO*, *HOXA*, *TLX3*, *TLX1*, *NKX2-1/2-2,* or *MEF2C*, in 80% of cases. Two patients with translocations of the *LMO3* transcription factor were identified, suggesting that *LMO3* activation may serve as an alternative to *LMO1/LMO2* activation in the pathogenesis of this disease. Moreover, intra-chromosomal rearrangements involving the 10q24 locus were found as a new mechanism of *TLX1* activation. An unequal distribution of cooperating genetic defects was found among the six genetic subgroups. Interestingly, deletions targeting *TCF7* or *TP53* were exclusively found in *HOXA* T-ALL, *LEF1* defects were prevalent in *NKX2-1* rearranged patients, *CASP8AP2* and *PTEN* alterations were significantly enriched in *TAL/LMO* leukemias whereas *PTPN2* and *NUP214-ABL1* abnormalities occurred in *TLX1/TLX3*. This work convincingly shows that CI-FISH is a powerful tool to define genetic heterogeneity of T-ALL which may be applied as a rapid and accurate diagnostic test.

Introduction

T-cell acute lymphoblastic leukemia (T-ALL) is a rare leukemia subtype, accounting for 15% of pediatric and 25% of adult ALL.[1] The disease is heterogeneous at the clinical and biological level and, mainly in adults, is characterized by a poor response to chemotherapy.[2] In the updated WHO classification[3] T-ALL is defined only by morphological features and immunophenotype, without inclusion of molecular-cytogenetic criteria to classify T-ALL patients into specific genetic entities. However, gene expression profiling (GEP) has shown that T-ALL comprises distinct subgroups, according to the level of expression of (onco)genes coding for transcription factors critical in hematopoiesis and/or T-cell development, maturation, and differentiation, ie, TAL/LMO, HOXA, TLX3, TLX1, NKX2-1/2-2, MEF2C (Type A abnormalities).[4-7] Furthermore, GEP has also identified an immature gene expression signature, which characterizes a specific subtype of T-ALL, termed early T-cell precursor ALL (ETP-ALL). In these cases, the leukemic blasts express myeloid/stem cell antigens (ie CD34/CD117, CD13, and/or CD33), whereas they are negative for CD1a, CD4, and CD8, and negative or weakly positive for CD5.[8] Although ETP-ALL have common immunophenotypic and expression markers, their genomic background appears largely heterogeneous with involvement of multiple T-lymphoid and myeloid genes.[8,9]

In addition to Type A abnormalities, integrated genomic analysis has uncovered a number of additional aberrations, including activating and inactivating mutations, chromosomal gains and losses, and balanced/unbalanced translocations. These events, herein referred to as Type B, involve epigenetic factors, ribosomal proteins, and proteins that belong to signaling pathways, such as JAK/STAT, RAS, WNT, and PI3K/AKT.[1,5,6,9-11] They occur non-randomly, in close association with the primary genetic changes, indicating that

specific concurrent events are required for leukemic development and expansion within each group.[10-15]

Due to the large number of genes and the variability of molecular mechanisms underlying their deregulation, more than one technological approach is usually required for complete genetic characterization of T-ALL. Thus, translation of bio-molecular information into routine diagnostics and clinical practice has remained challenging, and as a result, comprehensive, prospective studies within clinical trials are lacking. Nevertheless, genetic markers, especially if combined with minimal residual disease (MRD) quantification, may fine tune individual risk stratification and assist in predicting sensitivity to new drugs.[16-25] The French group FRALLE [20] demonstrated that persistence of MRD after induction, together with unfavorable genetic characteristics, including *N/K-RAS* mutations and *PTEN* alterations, improved risk assessment. Other examples include *MYC* translocations[12] as well as the absence of *CDKN2A* deletions,[21] which both appeared to identify high risk T-ALL subgroups. Moreover, preclinical studies have highlighted that deregulation of specific molecular targets, such as *NOTCH1*[21] and *JAK/STAT*[23] pathways, *BCL2*[24], *PIM1*[25], and *IL7R*[26] oncogenes, predicted sensitivity to specific inhibitors.

The aim of this study was to design a comprehensive interphase fluorescence *in situ* hybridization (CI-FISH) test as a robust and comprehensive diagnostic molecular-cytogenetic tool, to investigate known Type A and recurrent Type B genetic changes. Validation in retrospective cohorts of pediatric and adult patients enabled accurate genetic classification in 80% of cases and identified targetable lesions in approximately 85%.

Materials and Methods

Study cohort

A total of 338 T-ALL patients, enrolled onto the UK (MRC) and Italian (GIMEMA and AIEOP) clinical trials, were included in this study (**Table 1**). All patients or their parents/guardians gave informed consent for sample collection and molecular analyses, in agreement with the Declaration of Helsinki. The study was approved by the local bio-ethical committee (research project 3397/18). There were 225 children and 113 adults, with a male/female ratio of 2.8 (males 250; females 88). According to the immunophenotype, 223 cases were classified as ETP/near-ETP (n=45) or non-ETP (n=178) (Supplemental Table S1). Previously identified *NOTCH1/FBXW7* mutations were present in 139/215 patients investigated. The panel of genes involved in T-ALL were inferred from available gene expression profile, molecular cytogenetics, and sequencing data.[4-6,9,10] CI-FISH studies were performed in a two-step diagnostic algorithm (**Figure 1**).[16,27]

FISH probes

DNA clones were selected to study 21 oncogenes, whose genomic rearrangements were known to impact on *TAL/LMO, HOXA, TLX1, TLX3, MEF2C*, or *NKX2-1* deregulation, for classification of cases into these specific subgroups (Supplemental Table S2). An additional 49 genomic clones were chosen for investigation of genomic imbalances and/or translocations involving other T-ALL related genes/loci (Supplemental Table S3). For each gene/locus, clones were selected according to the type(s) of cytogenetic abnormalities under investigation. Break-apart probe sets were designed to study structural rearrangements, such as translocations, tandem duplications, and inversions, involving promiscuous genes. To investigate deletions involving oncosuppressor genes, BAC and/or fosmids, spanning the entire or part of a gene, were used (Supplemental Tables S2, S3, and S4).

To characterize the fusion partners of promiscuous genes, for example *MLLT10* with *PICALM, DDX3X, HNRNPH1,* or *NAP1L1*, *NUP214* with *SET, SQSTM1,* or *ABL1*, *NUP98* with *RAP1GDS1* or *PSIP1*, and *KMT2A* with *MLLT10, MLLT1, ELL, AFF1,* or *AFDN*, dual color dual fusion probe sets were designed (Supplemental Table S4). A specific dual color break-apart assay was designed (**Figure 2A, 2B, 2C, 2D**) to characterize *TLX1* intrachromosomal rearrangements in six patients (UPNs: PGTALL106, PGTALL160, PGTALL195, PGTALL209, PGTALL215, and PGTALL275). Commercial probes were used to study centromeric regions of selected chromosomes, to rule out numerical chromosomal changes. In all cases harboring a monoallelic *ETV6* deletion, *CDKN1B*, an oncosuppressor gene mapping 800Kb centromeric of *ETV6,* was also tested.

Directly-labeled FISH probes were designed from Bacterial Artificial Chromosomes (BACs; RPCI-11 Human Male BAC Library and Caltech BAC CTB, CTC and CTD Libraries), P1 derived Artificial Chromosomes (PACs; RPCI-1 and RPCI-5 Human Male PAC Library), and Fosmids (WIBR-2 Human Fosmid Library) (National Center for Biotechnology Information, https://www.ncbi.nlm.nih.gov/genome/gdv/; UCSC Genome Browser, University of California Santa Cruz, https://genome.ucsc.edu/) (last accessed July 30th, 2019). Bacterial clones were cultured in Luria-Bertani (LB) medium containing antibiotics; plasmid DNA was extracted using Qiagen Plasmid Midi Kit (Qiagen, Hilden, Germany) according to the manufacturer's instructions. DNA was labeled by Nick Translation Kit (Abbott Molecular, Des Plaines, IL) using SpectrumOrange dUTP, SpectrumGreen dUTP, and SpectrumAqua dUTP Vysis (Abbott Molecular). Dual or triple color assays were designed by combining differentially labeled probes into a ready-to-use working solution.

FISH protocol

Briefly, after labeling, probes were re-suspended in 10% dextran sulfate-50% formamide-4xSSC hybridization mixture with 20 ug of Human Cot-1 DNA Invitrogen (Fisher Scientific,

Milano, Italy). Slides were prepared from diagnostic peripheral blood (PB) and/or bone marrow (BM) cytogenetic pellets, spotted in 6 to 8 round areas on each slide. Slides were pretreated in a Coplin jar with protease solution (Dulbecco's Phosphate-Buffered Saline (DPBS)-0.01M HCl-0.01% pepsin) at 37 ℃ for 30 min, rinsed with DPBS at room temperature (RT) for 5 min and fixed in DPBS-4% formaldehyde/0,05M $MgCl_2$ at RT for 8 min. After a post-fixation wash with DPBS, slides were dehydrated through a cold ethanol series (70%-85%-100%) of 2 min each. Hybridization mix was applied to slides (3 microliter to each area), areas were covered by a round 10 mm coverslip and sealed with rubber cement. Slides and probes were co-denaturated on a hot plate at 76 ℃ for 10 minutes, hybridized over-night in moist chamber at 37 ℃, and washed with 0.4xSSC-0.3% Nonidet P-40 (Sigma-Aldrich, Saint Louis, MO) at 74 ℃, 2 min, and at RT, 2 min. Slides were counterstained with DAPI (0.5 microliter 0.1% DAPI in 1 mL Vectashield mounting medium, Vector Laboratories, Burlingame, CA), 30 microliter each slide. Between 120 to 200 nuclei were analyzed using a fluorescence microscope: Olympus BX61 (Olympus, Milano, Italy). When available, abnormal metaphases were analyzed using a highly sensitive camera JAI (Copenhagen, Denmark) and the image analysis software CytoVision 4.5.4 (Leica Microsystems, Wetzlar, Germany).

Abnormal hybridization patterns were: i) split signal (one fusion signal and separate green and red signals), ii) tandem duplication/trisomy (three signals), iii) deletion/monosomy (one signal), and iv) partial deletion (one fusion signal and one orange or one green signal). The cut-offs for the false positive detection of abnormal clones were set at the upper values of abnormal patterns seen in 10 peripheral blood samples from healthy donors, from scoring 200 nuclei for each sample. Split/duplication/trisomy patterns were considered to be positive when found in ≥3% of interphase cells; monosomy/deletion/partial deletion when

found in ≥6%. As the atypical hybridization pattern with multiple signals (>5) was never observed in normal controls, the cut-off levels for amplification was set at ≥0.5%.

Statistical analysis

Chi-square and Fisher exact tests (IBM SPSS 20) were used to analyze the distribution of Type A abnormalities according to age and phenotype, and to assess the correlation between recurrent Type B aberrations, the six main genetic subgroups, and phenotype.

Shallow whole-genome sequencing

Shallow whole-genome sequencing (sWGS)[28] is a low coverage next-generation sequencing technique, that has been designed to identify copy number variations. It was performed to characterize cases PGTALL215 and PGTALL2759 (Supplemental Table S1) which showed atypical hybridization patterns with the break-apart assay for the TLX1 gene, as previously described.[28] The amplified fragments were sequenced on the HiSeq 3000 (Illumina Inc.), according to the manufacturer's instructions. The minimal number of reads per sample was set at 10 million (mean coverage of 0.4×). Using a bin size of 100 kb, the R-Bioconductor package QDNAseq[29] was applied to visualize the DNA copy-number profile and call genomic aberrations. Each genome profile (line view and chromosome view) was manually checked for genomic abnormalities. All profiles were visualized using the online tool ViVar (http://cmgg.be/vivar/; last accessed July 30th, 2019).[30]

Results

Rearrangements and clonality

In a two-step diagnostic work-flow (**Figure 1**), CI-FISH detected 890 abnormalities within 96% of cases (=325), with a median and a mean of 3 per case (range: 1 to 8). No chromosomal aberrations were identified in 13 cases that displayed a normal hybridization pattern with all the CI-FISH assays (Supplemental Table S1). Genomic imbalances were prevalent, including 455 deletions, 56 duplications, and nine amplifications. A total of 49 trisomies were detected, with the most frequent being gains of chromosomes 8 (n=17), 6 and 7 (n=6 cases each), 10 (n=5), 19 (n=4), and 4, 18, and 21 (n=3 each); only one monosomy (chromosome 18) was identified (PGTALL202, Supplemental Table S1). Balanced and unbalanced translocations accounted for 316 events and involved T-cell receptors in 117 cases. Numerical aberrations, consistent with tri- and tetra- ploidy, were observed in four cases. Clonal primary changes were observed in 15% to 97% of cells, in agreement with the level of peripheral blood/bone marrow (PB/BM) leukemic infiltration by morphology (data not shown). Secondary changes were detected either in the main clone or in subclones, at a varible percentage of 3% to 90%. In a single case (PGTALL4, Supplemental Table S1), a subclonal *NUP214-ABL1* amplification, was detected in 0.5% of cells.

Type A abnormalities

CI-FISH successfully classified 261 out of 326 T-ALL (80%) into one of the six established genetic categories, whereas 65 cases remained unclassified (**Table 1**). In 12 cases complete screening for abnormalities involving primary oncogenes was not possible due to the lack or poor quality of samples, for example low efficiency of CI-FISH experiment (more than 20% of cells lacking hybridization signals), insufficient material, and/or weak hybridization signals.

TAL/LMO was the most highly represented group, comprising 89 positive cases. Genomic abnormalities classifying cases within the *TAL/LMO* group, involved *TAL1* (n=49), *LMO2* (n=19), *TAL2* (n=7), *LMO1* (n=5), *TAL1* and *LMO1/2* (n=6), *TAL1* and *LMO3* (n=1), *LMO3* (n=1) (**Figure 2E, 2F**), and *LYL1* with *LMO2* (n=1) (Supplemental Table S1). The *HOXA* subgroup comprised 76 cases, harboring translocations of *MLLT10* (n=24), *HOXA* (n=22), *NUP214* (n=10), *KMT2A* (n=10), and *NUP98* (n=9). In one case (UPN PGTALL 30) both *PICALM-MLLT10* and *TRG-HOXA* rearrangements were present (Supplemental Figure S1). *TLX3* rearrangements were found in 50 cases and involved various partners: *BCL11B* (n=37), *CDK6* (n=2), or undetermined (n=11).

TLX1 was involved in balanced (n=23) or unbalanced (n=4) rearrangements with *TR@* (n=19), or non-*TR@* partners (n=8). Six of the latter cases had intrachromosomal rearrangements: a cryptic deletion (PGTALL215), paracentric inversions (PGTALL106, PGTALL160, PGTALL195, PGTALL209) or paracentric inversion with accompanying deletions (PGTALL275) (see below). Notably, all of these intrachromosomal rearrangements resulted in the juxtaposition of *TLX1* close to regulatory sequences (chr10: 92,668,000-92,770,000) located ~10Mb upstream of its 5' end (http://asntech.org/dbsuper/index.php; http://www.enhanceratlas.org;https://enhancer.lbl.gov; last accessed July 30th, 2019).

The 17 cases assigned to the *NKX2-1* group harbored translocations of *NKX2-1* (n=15), *NKX2-2* (n=1), or *MYB* (n=1). Lastly, *SPI.1* and *RUNX1* translocations, both underlying *MEF2C* over-expression,[6] were detected in one child and one adult, respectively.

Patients were allotted to the main categories based on age ($P < 0.001$) (**Figure 2G**). The higher prevalence of *TAL/LMO* (40% vs 22%; $P= 0.0007$) and *TLX3* (23% vs 10%; $P= 0.0092$) in children and, of *TLX1* in adults (5% vs 22%; $P=0.0005$), confirmed previous reports. Two novel findings which emerged from this study were the significant association

of the *NKX2-1/2-2* group with childhood (9% vs 1%; *P* = 0.0083), and of *HOXA* with adult T-ALL (44% vs 22%; *P* = 0.0061). Correlating the genetic groups with phenotypes, *HOXA* was the most highly represented group in ETP/ETP-like ALL (46.3% of cases; *P* < 0,001) (**Figure 2G**).

Characterization of intrachromosomal rearrangements of TLX1

The hybridization pattern of the *TLX1* probe set RP11-108L7 (centromeric to *TLX1*) and RP11-107I14 (telomeric to *TLX1*) (Supplemental Table S2) not only detected balanced *TLX1* translocations, but also two new rearrangements. Namely, in cases PGTALL106 (**Figure 2B**), PGTALL160, PGTALL195, and PGTALL209 (**Figure 2C**), the hybridization pattern was consistent with a paracentric inversion, whereas in cases PGTALL215 and PGTALL275 (**Figure 2D**), a cryptic deletion was found at the centromeric side of the gene. In these two latter cases, sWGS confirmed two different genomic losses at 10q23, and precisely indicated their smaller extent (Supplemental Figure S2). The break-apart FISH probe set (RP11-641A1 and RP11-703D23), specifically designed to characterize the centromeric breakpoints of these intrachromosomal rearrangements (**Figure 2A**), showed that both inversions and deletions shared the same breakpoint, ~10Mb centromeric of *TLX1* that placed *TLX1* in close proximity to known enhancer sequences (**Figure 2A, 2B, 2C, 2D**).

Recurrent Type B abnormalities and their distribution

Type B aberrations were detected in 87% of classified (229/262), 81% of unclassified cases (53/65), and 91% of cases for which screening for primary changes was incomplete (11/12) (Supplemental Table S1). Amongst them, 17 genomic rearrangements, including partial chromosomal losses and gains or balanced translocations, and three chromosomal trisomies, were considered to be recurrent as they were found in five or more cases (**Table**

2). An unequal distribution of cooperating genetic defects was also identified over the different genetic subtypes (**Figure 3**).

Chromosome deletions

One or more deletions were found in 79% of cases (267/338). Overall, the most frequently deleted genes/loci were: *CDKN2AB* (63%), *CASP8AP2* (13%), *PTEN* (8%), *LEF1* (8%), *TCF7* (7%), *PTPN2* (7%), *NF1/SUZ12* (6%), and *ETV6* (6%) (**Table 2**). Deletions of *CDKN2AB*, including mono- and/or bi- allelic, partial or complete, were found in 76% to 85% of *TAL/LMO*, *TLX1/3*, and *NKX2-1/2-2*, but only in 42% of *HOXA* positive cases (*P* < 0,001). Within the *HOXA* group, *CDKN2AB* deletions were detected in 50% of non-ETP and 31.5% of ETP cases. Deletions of 6q were the second most frequent losses (47/324). Widely heterogeneous, they involved chromosomal bands 6q14 to 6q23 and encompassed the oncosuppressor *CASP8AP2*/6q14 in 41 cases (~13%) (Supplemental Table S5). Loss of *CASP8AP2* was significantly associated with the *TAL/LMO* group (*P* = 0.01). *PTEN* deletions occurred in 8% of the entire study cohort, but were enriched within the *TAL/LMO* subgroup, in 19% of positive cases (*P* = 0.05). *ETV6* deletions co-occurred with *CDKN1B* deletions in all cases and were significantly associated with *TLX1,* whereas *PTPN2* deletions were enriched within both *TLX1* and *TLX3* groups. Loss of *LEF1* and *BCL11B* were highly recurrent in the *NKX2-1/2-2* subgroup. Lastly, genomic losses of *TCF7* and *TP53* were exclusively found in the *HOXA* subgroup.

Gains/amplifications and trisomies

Recurrent genomic gains involved *MYB* and a 9q34 region of variable size. Three copies of *MYB* were detected in 14 cases (5%), which resulted from tandem duplication (n=11) or large 6q duplications (n=3); dup(9)(q34) involved *NOTCH1*, *NUP214, ABL1,* and/or *TAL2*,

and showed no specific association with the main genetic subgroups. Unique recurrent amplifications involved the *NUP214-ABL1* fusion gene in eight cases, seen as extra- and intra- chomosomal in five and three cases, respectively. The *NUP214-ABL1* rearrangement was found in highly variable clone sizes, ranging from 0.5% to 100%, and were confined to the *TLX* (*TLX1* 4% and *TLX3* 12%) and *HOXA* (1%) categories.

Balanced translocations

The most recurrent balanced translocations involved the *MYC* oncogene (15/306; 5% of cases), with *TR*@ (n=7) or non-*TR*@ (n=8) partners. Rare translocations/rearrangements, occuring in less than 1% of cases, involved *JAK2* (PGTALL50, PGTALL59, PGTALL144), *CCND2* (PGTALL63, PGTALL172), and *ETV6* (PGTALL69, PGTALL234) (Supplemental Table S1).

Discussion

The CI-FISH assay was successfully applied in pediatric and adult T-ALL, and identified an abnormal signal pattern in almost all cases (98%) allowing genetic classification in 80% of them. Compared to single-nucleotide polymorphism (SNP) array, CI-FISH was more accurate in identification of small clonal/subclonal changes, thus providing a more favorable approach for genetic classification of T-lymphoblastic lymphomas (T-LBL), in which bone marrow leukemic infiltration is ≤25%.[3] Moreover, SNP array detection is limited to unbalanced rearrangements, characterized by partial chromosomal gains and losses, whereas CI-FISH clearly identified balanced changes that are undetected by SNP array. However it is worth noting that an integrated approach including SNP array, with next-generation techniques, for example whole genome, exome,

and RNA sequencing, provided accurate genetic classification in 91% of childhood T-ALL.[10] Although sequencing approaches will likely replace molecular cytogenetics in the future, as it provides information on the entire genomic landscape of sequence variants, currently diagnostic laboratories are still better equipped to perform FISH.

Besides detecting all known Type A abnormalities, CI-FISH unveiled new targets and new mechanisms of gene deregulation by identifying cryptic chromosomal aberrations, new *TR@* rearrangements and gene promiscuity. As expected for early events, Type A abnormalities were always present in the main clone in a percentage of positive cells consistent with the degree of BM/PB leukemic infiltration. Overall, 80% of cases were classified into one of the six major genetic groups, ie, *TAL/LMO*, *HOXA*, *TLX1*, *TLX3*, *NKX2-1*, and *MEF2C*.[4-8,10]

The *HOXA* subgroup first emerged as significantly associated with adult T-ALL. However, here, its significant association with ETP/near-ETP phenotype was also confirmed (**Figure 2G**).[5,31]

Two additional significant associations were the previously known association of *TLX1* in adults and the newly emerged link between the *NKX2-1* subgroup and childhood T-ALL. Interestingly, these two subgroups share a cortical thymocytic arrest and a similar/overlapping gene expression profiling[6] suggesting that the two oncogenes mark closely related leukemogenic entities occurring in distinct patient's age groups.

Interestingly, as the testing of primary oncogenes was expanded to all four members of the rhombotin family of cysteine-rich LIM domain genes, not only *LMO1* and *LMO2*, but also *LMO3* was found to be recurrently involved in *TRB* translocations in T-ALL (**Figure 2E, 2F**). *LMO3* shares structural and functional homology with the other family members, and has been found to act as an oncogene in neuroblastoma.[32] Normally

silenced in T-lymphocytes, *LMO3* has been already reported as a new leukemogenic target in T-ALL, resulting from the t(7;12)(q34;p13) translocation which positions the *TRB* enhancer in close proximity to *LMO3* leading to its transcriptional activation.[33] Based on the structural similarities between the three members of the *LMO* family,[34,35] as well as the association of both *LMO1/2* and *LMO3* with *SIL-TAL1*, our interpretation was that cases with *TRB-LMO3* likely belong to the *TAL/LMO* group.

Another discovery was that approximately 30% of *TLX1* rearrangements were independent from *TR@* translocations. The majority of these non-*TR@* abnormalities involved paracentric inversions and/or cryptic interstitial deletions that invariably juxtaposed *TLX1* to nearby regulatory sequences within 10q23. Of note, these cases shared the same 10q23 breakpoints reported by Liu et al[10] in ~29% of pediatric *TLX1*-positive T-ALL, thus indicating that intra-chromosomal rearrangements are the second most frequent mechanism underlying *TLX1* transcriptional activation (**Figure 2A**).

Another noteworthy finding was the higher percentage of *HOXA* positive cases than previously reported in both children[5] and adults,[36] probably because CI-FISH has the capacity to detect translocations involving the full range promiscuous genes leading to *HOXA* expression. Interestingly, one *HOXA* positive leukemia case was found to carry two primary hits: *PICALM-MLLT10* and *TRG-HOXA* within the same leukemic clone (Supplemental Figure S1).[37] The novelty of this case lies in the involvement of the *TRG* locus as a recurrent translocation partner of T-ALL–related oncogenes.[38] The involvement of TRG should be tested for future molecular-cytogenetic assays, especially to elucidate as yet unknown mechanisms of gene deregulation and prognostic biomarkers.

In keeping with the accepted model of a multistep leukemogenic process, CI-FISH detected multiple *Type B* aberrations, confirming that accumulation of several abnormalities are necessary for disease progression and for informing on specific

associations between different cooperative events. Overall, at least one actionable pathway was identified in approximately 85% of cases (**Table 2 and Figure 3**). The most frequent rearrangements included genes involved in cell cycle/apoptosis, (*CDKN2A, CDKN1B, CASP8AP2, RB1*, and *TP53*; 65%), *WNT* (*LEF1, MYC* 13%), *PI3K/AKT* (*PTEN* 8%), *JAK/STAT* (*PTPN2, NUP214-ABL1* 8%), and *RAF/MEK/ERK* (*NF1* 6%) signaling pathways, or of the epigenetic complex *PRC2* (*SUZ12* 6%). Preferential associations were corroborated between primary and secondary changes, such as that of *PTEN* and *MYC* with *TAL/LMO* and *NUP214-ABL1* and *PTPN2* with *TLX1/3.*[9-15] Interestingly, previously unknown combinations, such as *TCF7* and *TP53* deletions in *HOXA* positive cases or *LEF1* in the *NKX2-1* group, were demonstrated. Specific links were also observed between secondary changes and an immature phenotype. As expected, *NOTCH/FBXW7* mutations and *CDKN2AB* deletions were under-represented in the ETP/near-ETP ALL group which, on the other hand, showed a high incidence of *TCF7*, *WT1*, *ETV6*, *RB1*, *NF1*, and *TP53* deletions (Supplemental Table S6). In addition to genomic rearrangements, mutations of members/modulators of the *NOTCH* pathway (*NOTCH1* and/or *FBXW7*), were detected in 65% of the cases. As previously reported by Zuurbier et al,[39] a significant lower frequency of *NOTCH1/FBXW7* mutations was found in cases belonging to the *TAL/LMO* subgroup (**Table 2**), which, on the other hand, showed a closer link with the *PI3K/AKT* pathway (19% of *PTEN* deletions vs 8% in the overall cohort, $P = 0,05$).[10,40]

Taken together, these findings confirmed that the synergistic effect of specific deregulated genes/pathways is necessary for leukemia onset, maintenance, and progression, suggesting that identification of multiple specific targets,[22-26,41] within the same leukemia sample, should be considered for combinatorial therapeutic intervention.[42-44]

Conclusion

In T-ALL, genetic markers have not yet been integrated into risk stratification and for treatment options, as a complementary approach to the standard evaluation of minimal residual disease. The translation of molecular findings into clinical practice remains challenging due to the genetic complexity and heterogeneity of T-ALL and the observation that focusing on single markers can provide misleading information.[45]

One major issue has been the identification of the most convenient diagnostic approach for the detection of these multiple heterogenous concurrent events in individual patients and to select the most reliable markers/pathways to be exploited in treatment and monitoring. This study highlighted CI-FISH as a powerful assay in the diagnostic work-up of pediatric and adult T-ALL and T-LBL. Coupled with targeted sequencing of recurrently mutated genes, it provides comprehensive genetic diagnosis of T-ALL for detection of actionable bio-markers in the context of clinical trials.

Acknowledgments

We thank Donatella Beacci and Silvia Romoli for their help in the preparation of biological samples.

References

1. Girardi T, Vicente C, Cools J, De Keersmaecker K: The genetics and molecular biology of T-ALL. Blood 2017, 129:1113-1123
2. Marks DI, Rowntree C: Management of adults with T-cell lymphoblastic leukemia. Blood 2017, 129:1134-1142
3. Borowitz MJ, Chan JK, Dowing JR, Le Beau MM, Arber. WHO Classification of Tumours of Haematopoietic and Lymphoid Tissues: Precursor Lymphoid neoplasm. Edited by IARC Lyon 2017, pp 199-213.
4. Ferrando AA, Neuberg DS, Staunton J, Loh ML, Huard C, Raimondi SC, Behm FG, Pui CH, Downing JR, Gilliland DG, Lander ES, Golub TR, Look AT: Gene expression signature define novel oncogenic pathways in T cell acute lymphoblastic leukemia. Cancer Cell 2002, 1:75-87
5. Belver L, Ferrando A: The genetics and mechanisms of T cell acute lymphoblastic leukaemia. Nat Rev Cancer 2016, 16:494-507
6. Homminga I, Pieters R, Langerak AW, de Rooi JJ, Stubbs A, Verstegen M, Vuerhard M, Buijs-Gladdines J, Kooi C, Klous P, van Vlierberghe P, Ferrando AA, Cayuela JM, Verhaaf B, Beverloo HB, Horstmann M, de Haas V, Wiekmeijer AS, Pike-Overzet K, Staal FJ, de Laat W, Soulier J, Sigaux F, Meijerink JP: Integrated transcript and genome analyses reveal NKX2-1 and MEF2C as potential oncogenes in T cell acute lymphoblastic leukemia. Cancer Cell 2011, 19:484-497
7. Van Vlierberghe P, Pieters R, Beverloo HB, Meijerink JP. Molecular-genetic insights in paediatric T-cell acute lymphoblastic leukaemia. British Journal Haematology 2008; 143:153-68
8. Coustan-Smith E, Mullighan CG, Onciu MM, Behm FG, Raimondi SC, Pei D, Cheng C, Su X, Rubnitz JE, Basso G, Biondi A, Pui CH, Downing JR, Campana D: Early T-

cell precursor leukemia: a subtype of very risk acute lymphoblastic leukemia identified in two independent cohorts. The Lancet Oncology 2009, 10:147-156

9. Zhang J, Ding L, Holmfeldt L, Wu G, Heatley SL, Payne-Turner D, Easton J, Chen X, Wang J, Rusch M, Lu C, Chen SC, Wei L, Collins-Underwood JR, Ma J, Roberts KG, Pounds SB, Ulyanov A, Becksfort J, Gupta P, Huether R, Kriwacki RW, Parker M, McGoldrick DJ, Zhao D, Alford D, Espy S, Bobba KC, Song G, Pei D, Cheng C, Roberts S, Barbato MI, Campana D, Coustan-Smith E, Shurtleff SA, Raimondi SC, Kleppe M, Cools J, Shimano KA, Hermiston ML, Doulatov S, Eppert K, Laurenti E, Notta F, Dick JE, Basso G, Hunger SP, Loh ML, Devidas M, Wood B, Winter S, Dunsmore KP, Fulton RS, Fulton LL, Hong X, Harris CC, Dooling DJ, Ochoa K, Johnson KJ, Obenauer JC, Evans WE, Pui CH, Naeve CW, Ley TJ, Mardis ER, Wilson RK, Downing JR, Mullighan CG: The genetic basis of early T-cell precursor acute lymphoblastic leukaemia. Nature 2012, 481:157-163
10. Liu Y, Easton J, Shao Y, Maciaszek J, Wang Z, Wilkinson MR, McCastlain K, Edmonson M, Pounds SB, Shi L, Zhou X, Ma X, Sioson E, Li Y, Rusch M, Gupta P, Pei D, Cheng C, Smith MA, Auvil JG, Gerhard DS, Relling MV, Winick NJ, Carroll AJ, Heerema NA, Raetz E, Devidas M, Willman CL, Harvey RC, Carroll WL, Dunsmore KP, Winter SS, Wood BL, Sorrentino BP, Downing JR, Loh ML, Hunger SP, Zhang J, Mullighan CG: The genomic landscape of pediatric and young adult T-lineage acute lymphoblastic leukemia. Nat Genet 2017, 49:1211-1218
11. Durinck K, Goossens S, Peirs S, Wallaert A, Van Loocke W, Matthijssens F, Pieters T, Milani G, Lammens T, Rondou P, Van Roy N, De Moerloose B, Benoit Y, Haigh J, Speleman F, Poppe B, Van Vlierberghe P: Novel biological insights in T-cell acute lymphoblastic leukemia. Exp Hematol 2015, 43:625-639
12. La Starza R, Borga C, Barba G, Pierini V, Schwab C, Matteucci C, Lema Fernandez AG, Leszl A, Cazzaniga G, Chiaretti S, Basso G, Harrison CJ, Te Kronnie G,

Mecucci C: Genetic profile of T-cell acute lymphoblastic leukemias with MYC translocations. Blood 2014, 124:3577-3582

13. La Starza R, Barba G, Demeyer S, Pierini V, Di Giacomo D, Gianfelici V, Schwab C, Matteucci C, Vicente C, Cools J, Messina M, Crescenzi B, Chiaretti S, Foà R, Basso G, Harrison CJ, Mecucci C: Deletions of the long arm of chromosome 5 define subgroups of T-cell acute lymphoblastic leukemia. Haematologica 2016, 101:951-958
14. La Starza R, Messina M, Gianfelici V, Pierini V, Matteucci C, Pierini T, Limongi MZ, Vitale A, Roti G, Chiaretti S, Foà R, Mecucci C: High PIM1 expression is a biomarker of T-cell acute lymphoblastic leukemia with JAK/STAT activation or t(6;7)(p21;q34)/TRB@-PIM1 rearrangement. Leukemia 2018, 32:1807-1810
15. Vicente C, Schwab C, Broux M, Geerdens E, Degryse S, Demeyer S, Lahortiga I, Elliott A, Chilton L, La Starza R, Mecucci C, Vandenberghe P, Goulden N, Vora A, Moorman AV, Soulier J, Harrison CJ, Clappier E, Cools J: Targeted sequencing identifies associations between IL7R-JAK mutations and epigenetic modulators in T-cell acute lymphoblastic leukemia. Haematologica 2015, 100:1301-1310
16. La Starza R, Lettieri A, Pierini V, Nofrini V, Gorello P, Songia S, Crescenzi B, Te Kronnie G, Giordan M, Leszl A, Valsecchi MG, Aversa F, Basso G, Biondi A, Conter V, Cazzaniga G, Mecucci C: Linking genomic lesions with minimal residual disease improves prognostic stratification in children with T-cell acute lymphoblastic leukaemia. Leuk Res 2013, 37:928-935
17. O'Connor D, Enshaei A, Bartram J, Hancock J, Harrison CJ, Hough R, Samarasinghe S, Schwab C, Vora A, Wade R, Moppett J, Moorman AV, Goulden N: Genotype-Specific Minimal Residual Disease Interpretation Improves Stratification in Pediatric Acute Lymphoblastic Leukemia. J Clin Oncol 2018, 36:34-43

18. Richter-Pechańska P, Kunz JB, Hof J, Zimmermann M, Rausch T, Bandapalli OR, Orlova E, Scapinello G, Sagi JC, Stanulla M, Schrappe M, Cario G, Kirschner-Schwabe R, Eckert C, Benes V, Korbel JO, Muckenthaler MU, Kulozik AE: Identification of a genetically defined ultra-high-risk group in relapsed pediatric T-lymphoblastic leukemia. Blood Cancer J 2017, 7:e523
19. Ferrando A: NOTCH mutations as prognostic markers in T-ALL. Leukemia. 2010, 24:2003-2004
20. Petit A, Trinquand A, Chevret S, Ballerini P, Cayuela JM, Grardel N, Touzart A, Brethon B, Lapillonne H, Schmitt C, Thouvenin S, Michel G, Preudhomme C, Soulier J, Landman-Parker J, Leverger G, Macintyre E, Baruchel A, Asnafi V; French Acute Lymphoblastic Leukemia Study Group (FRALLE): Oncogenetic mutations combined with MRD improve outcome prediction in pediatric T-cell acute lymphoblastic leukemia. Blood 2018, 131:289-300
21. Genescà E, Lazarenkov A, Morgades M, Berbis G, Ruíz-Xivillé N, Gómez-Marzo P, Ribera J, Juncà J, González-Pérez A, Mercadal S, Guardia R, Artola MT, Moreno MJ, Martínez-López J, Zamora L, Barba P, Gil C, Tormo M, Cladera A, Novo A, Pratcorona M, Nomdedeu J, González-Campos J, Almeida M, Cervera J, Montesinos P, Batlle M, Vives S, Esteve J, Feliu E, Solé F, Orfao A, Ribera JM: Frequency and clinical impact of CDKN2A/ARF/CDKN2B deletions as assessed by in-depth genetic analysis in adult T cell acute lymphoblastic leukemia. J Hematol Oncol 2018, 11:96
22. Roti G, Stegmaier K: New approaches to target T-ALL. Front Oncol 2014, 4:170
23. Maude SL, Dolai S, Delgado-Martin C, Vincent T, Robbins A, Selvanathan A, Ryan T, Hall J, Wood AC, Tasian SK, Hunger SP, Loh ML, Mullighan CG, Wood BL, Hermiston ML, Grupp SA, Lock RB, Teachey DT: Efficacy of JAK/STAT pathway

inhibition in murine xenograft models of early T-cell precursor (ETP) acute lymphoblastic leukemia. Blood 2015, 125:1759-1767

24. Kawashima-Goto S, Imamura T, Tomoyasu C, Yano M, Yoshida H, Fujiki A, Tamura S, Osone S, Ishida H, Morimoto A, Kuroda H, Hosoi H : BCL2 Inhibitor (ABT-737): A Restorer of Prednisolone Sensitivity in Early T-Cell Precursor-Acute Lymphoblastic Leukemia with High MEF2C Expression. PLOS One 2015, 10:e0132926

25. De Smedt R, Peirs S, Morscio J, Matthijssens F, Roels J, Reunes L, Lintermans B, Goossens S, Lammens T, Van Roy N, Touzart A, Jenni S, Tsai YC, Lovisa F, Mussolin L, Serafin V, Van Nieuwerburgh F, Deforce D, Uyttebroeck A, Tousseyn T, Burkhardt B, Klapper W, De Moerloose B, Benoit Y, Macintyre E, Bourquin JP, Basso G, Accordi B, Bornhauser B, Meijerink J, Vandenberghe P, Van Vlierberghe P: Pre-clinical evaluation of second generation PIM inhibitors for the treatment of T-cell acute lymphoblastic leukemia and lymphoma. Haematologica 2019, 104:e17-e20

26. Li Y, Buijs-Gladdines JG, Canté-Barrett K, Stubbs AP, Vroegindeweij EM, Smits WK, van Marion R, Dinjens WN, Horstmann M, Kuiper RP, Buijsman RC, Zaman GJ, van der Spek PJ, Pieters R, Meijerink JP. IL-7 Receptor Mutations and Steroid Resistance in Pediatric T cell Acute Lymphoblastic Leukemia: A Genome Sequencing Study.PLoS Medicine 2016;13: e1002200

27. Gorello P, La Starza R, Varasano E, Chiaretti S, Elia L, Pierini V, Barba G, Brandimarte L, Crescenzi B, Vitale A, Messina M, Grammatico S, Mancini M, Matteucci C, Bardi A, Guarini A, Martelli MF, Foà R, Mecucci C: Combined interphase fluorescence in situ hybridization elucidates the genetic heterogeneity of T-cell acute lymphoblastic leukemia in adults. Haematologica 2010, 95:79-86

28. Van Roy N, Van Der Linden M, Menten B, Dheedene A, Vandeputte C, Van Dorpe J, Laureys G, Renard M, Sante T, Lammens T, De Wilde B, Speleman F, De Preter K: Shallow Whole Genome Sequencing on Circulating Cell-Free DNA Allows Reliable Noninvasive Copy-Number Profiling in Neuroblastoma Patients. Clinical Cancer Research 2017, 23:6305-6314

29. Scheinin I, Sie D, Bengtsson H, van de Wiel MA, Olshen AB, van Thuijl HF, van Essen HF, Eijk PP, Rustenburg F, Meijer GA, Reijneveld JC, Wesseling P, Pinkel D, Albertson DG, Ylstra B: DNA copy number analysis of fresh and formalin-fixed specimens by shallow whole-genome sequencing with identification and exclusion of problematic regions in the genome assembly. Genome Research, 2014, 24:2022-2032

30. Sante T, Vergult S, Volders PJ, Kloosterman WP, Trooskens G, De Preter K, Dheedene A, Speleman F, De Meyer T, Menten B: ViVar: A Comprehensive Platform for the Analysis and Visualization of Structural Genomic Variation. Plos One 2014, 9: e113800

31. Bond J, Marchand T, Touzart A, Cieslak A, Trinquand A, Sutton L, Radford-Weiss I, Lhermitte L, Spicuglia S, Dombret H, Macintyre E, Ifrah N, Hamel JF, Asnafi V: An early thymic precursor phenotype predicts outcome exclusively in HOXA-overexpressing adult T-cell acute lymphoblastic leukemia: a Group for Research in Adult Acute Lymphoblastic Leukemia study. Haematologica 2016, 101:732-740

32. Aoyama M, Ozaki T, Inuzuka H, Tomotsune D, Hirato J, Okamoto Y, Tokita H, Ohira M, Nakagawara A: LMO3 interacts with neuronal transcription factor, HEN2, and acts as an oncogene in neuroblastoma. Cancer Res 2006, 65:4587-4597

33. Simonis M, Klous P, Homminga I, Galjaard RJ, Rijkers EJ, Grosveld F, Meijerink JP, de Laat W: High-resolution identification of balanced and complex chromosomal rearrangements by 4C technology. Nat Method 2009, 6:837-842

34. Boehm T, Foroni L, Kaneko Y, Perutz MF, Rabbitts TH: The rhombotin family of cysteine-rich LIM-domain oncogenes: distinct members are involved in T-cell translocations to human chromosomes 11p15 and 11p13. PNAS 1991, 88:4367-4371

35. Sang M, Ma L, Sang M, Zhou X, Gao W, Geng C: LIM-domain-only proteins: multifunctional nuclear transcription coregulators that interacts with diverse proteins. Mol Biol Rep 2014, 41:1067-1073

36. Soulier J, Clappier E, Cayuela JM, Regnault A, García-Peydró M, Dombret H, Baruchel A, Toribio ML, Sigaux F: HOXA genes are included in genetic and biologic networks defining human acute T-cell leukemia (T-ALL). Blood 2005, 106:274-286

37. Bergeron J, Clappier E, Cauwelier B, Dastugue N, Millien C, Delabesse E, Beldjord K, Speleman F, Soulier J, Macintyre E, Asnafi V: HOXA cluster deregulation in T-ALL associated with both a TCRD-HOXA and a CALM-AF10 chromosomal translocation. Leukemia 2006, 20:1184-1187

38. Gesk S, Martın-Subero JI, Harder L, Luhmann B, Schlegelberger B, Calasanz MJ, Grote W, Siebert R: Molecular cytogenetic detection of chromosomal breakpoints in T-cell receptor gene loci. Leukemia 2003, 17:738–745

39. Zuurbier L, Homminga I, Calvert V, te Winkel ML, Buijs-Gladdines JG, Kooi C, Smits WK, Sonneveld E, Veerman AJ, Kamps WA, Horstmann M, Petricoin EF 3rd, Pieters R, Meijerink JP. NOTCH1 and/or FBXW7 mutations predict for initial good prednisone response but not for improved outcome in pediatric T-cell acute lymphoblastic leukemia patients treated on DCOG or COALL protocols. Leukemia 2010; 24:2014-2022

40. Zuurbier L, Petricoin EF3rd, Vuerhard MJ, Calvert V, Kooi C, Buijs-Gladdines JG, Smits WK, Sonneveld E, Veerman AJ, Kamps WA, Horstmann M, Pieters R,

Meijerink JP. The significance of PTEN and AKT aberrations in pediatric T-cell acute lymphoblastic leukemia. Haematologica 2012; 97:1405-1413

41. Bertacchini J, Heidari N, Mediani L, Capitani S, Shahjahani M, Ahmadzadeh A, Saki N: Targeting PI3K/AKT/mTOR network for treatment of leukemia. Cell Mol Life Sci 2015, 72:2337-2347
42. Peirs S, Matthijssens F, Goossens S, Capitani S, Shahjahani M, Ahmadzadeh A, Saki N: ABT-199 mediated inhibition of BCL-2 as a novel therapeutic strategy in T-cell acute lymphoblastic leukemia. Blood 2014, 124:3738-3747
43. Daigle SR, Olhava EJ, Therkelsen CA, Basavapathruni A, Jin L, Boriack-Sjodin PA, Allain CJ, Klaus CR, Raimondi A, Scott MP, Waters NJ, Chesworth R, Moyer MP, Copeland RA, Richon VM, Pollock RM: Potent inhibition of DOT1L as treatment of MLL-fusion leukemia. Blood 2013, 122:1017-1025
44. Deveau AP, Forrester AM, Coombs AJ, Wagner GS, Grabher C, Chute IC, Léger D, Mingay M, Alexe G, Rajan V, Liwski R, Hirst M, Steigmaier K, Lewis SM, Look AT, Berman JN: Epigenetic therapy restores normal hematopoiesis in a zebrafish model of NUP98-HOXA9-induced myeloid disease Leukemia 2015 29:2086-2097
45. Ma J, Wu M: The indicative effect of Notch1 expression for the prognosis of T-cell acute lymphocytic leukemia: a systematic review. Mol Biol Rep 2012, 39:6095-6100

Figure Legends

Figure 1. Schematic representation of the comprehensive fluorescence *in situ* hybridization (CI-FISH) flowchart applied to diagnostic samples of T-ALL. Cytogenetic pellets can be obtained after direct or 24 hour culturing. The first round provides information on Type A abnormalities and TR@ involvement in about four days; the second round detects additional recurrent abnormalities (Type B) in further four days. BM/PB, bone marrow/peripheral blood; TF, transcription factors. All tests are performed each time.

Figure 2. A: Schematic representation of the long arm of chromosome 10 with mapping of *TLX1* and DNA clones used to define the breakpoints (blue arrows) of paracentric inversions and cryptic deletions. **B:** Fluorescence *in situ* hybridization (FISH) in case PGTALL106 with paracentric inversion. **C:** FISH in case PGTALL209 with a cryptic deletion. **D:** FISH in case PGTALL275 with paracentric inversion and an accompayning deletion (white arrows indicate the abnormal hybridization patterns). **E:** Schematic representation of the short arm of chromosome 12 with mapping of *LMO3* and of the clones used in a break-apart assay. **F:** FISH in case PGTALL44 with *LMO3* translocation (arrows indicate split green/orange signals) (all FISH images were taken at 100x magnification). **G:** Pies show the distribution of the six main genetic groups according to the age (percentages were referred to the 261 classified cases, ie, 178 children and 83 adults) and to an immature phenotype (45 cases with ETP/near-ETP ALL).

Figure 3. The heat-map shows the distribution of Type B abnormalities according to the main genetic groups (*TLX1* and *TLX3* were grouped together; the two cases of *MEF2C* positive T-ALL were not included).

Table 1. Clinical and hematological features of our cohort of T-ALL.

	CHILDREN (n=225)	**ADULTS (n=113)**	**COHORT (n=338)**	***P*-value**
Age range (years)	3-18	19-78	3-78	
Median	10	35	15	
Media	10	35	35	
SEX				
Male	168	82	250	
Female	57	31	88	
PHENOTYPE		96	223	
Typical	110	68	178	
ETP	17	28	45	
WBC x 10^9/L	63	92	155	
<100	32	72	104	
≥100	31	20	51	
CLASSIFICATION	213	113	326	
TAL/LMO	71	18	89	0.0007
HOXA	40	36	76	0.0061
TLX3	41	9	50	0.0092
TLX1	9	18	27	0.0005
NKX2-1/2-2	16	1	17	0.0083
MEF2C	1	1	2	
Unclassified	35	30	65	
Failed	12	0	12	
Numerical changes	22	15	37	
Imbalances	180	92	272	

Tri- tetra- ploidy	3	1	4
Normal CI-FISH	10	3	13

WBC, white blood cells; ETP, early precursor T-cell acute lymphoblastic leukemia; Fisher exact tests (IBM SPSS 20) was used to evaluate distribution of the main genetic groups according to age.

Table 2. Recurrent secondary changes in 338 pediatric and adult T-ALL.

GENE/LOCUS	Overall	*TAL/LMO*	*HOXA*	*TLX3*	*TLX1*	*NKX2-1/2-2*	*MEF2C*	*P*-value*
CDKN2AB	63% (207/326)	67 (77%)	**31 (42%)**	38 (81%)	22 (85%)	13 (76%)	0	<0.001
CASP8AP2	13% (41/324)	**21 (24%)**	8 (11%)	1 (2%)	2 (11%)	3 (18%)	0	0.06
TP53	5% (9/165)	0	**6 (10%)**	0	0	0	0	NS
RB1	3% (6/217)	0	3 (5%)	1 (5%)	0	0	0	NS
PTEN	8% (27/333)	**17 (19%)**	3 (4%)	0	0	0	0	<0.001
PTPN2	7% (22/331)	0	3 (4%)	**9 (18%)**	**8 (30%)**	2 (12%)	0	<0.001
NUP214-ABL1	2% (8/325)	0	1 (1%)	**6 (12%)**	**1 (4%)**	0	0	0.001
NF1	6% (19/330)	0	5 (6%)	1 (2%)	0	0	1	<0.001
SUZ12	6% (19/330)	0	5 (6%)	1 (2%)	0	0	1	<0.001
NOTCH1/FBXW7	65% (139/215)	21 (44%)	38 (75%)	22 (81%)	12 (80%)	15 (94%)	2	<0.001
LEF1	8% (24/313)	9 (10%)	1 (1%)	2 (4%)	0	**5 (29%)**	0	0.003
MYC	5% (15/306)	9 (10%)	2 (3%)	1 (3%)	1 (4%)	0	0	NS
ETV6	6% (15/264)	0	5 (8%)	1 (3%)	**5 (25%)**	0	0	0.004
WT1	5% (14/259)	0	7 (11%)	5 (14%)	1 (5%)	0	0	0.005
BCL11B	3% (9/271)	1 (1%)	2 (3%)	0	2 (11%)	**3 (18%)**	0	0.012
IKZF1	3% (6/214)	0	1 (2%)	2 (6%)	0	1 (20%)	0	NS
MYB	5% (14/280)	2 (3%)	6 (10%)	2 (6%)	1 (4%)	0	0	NS
TCF7	7% (21/283)	0	**13 (21%)**	0	0	0	1	<0.001
DUP(9Q)	4% (14/332)	4 (5%)	3 (4%)	0	2 (7%)	1 (6%)	0	NS
Trisomy 8	5% (17/306)	3 (3%)	2 (3%)	2 (5%)	4 (16%)	0	0	NS
Trisomy 6	2% (6/280)	2 (3%)	3 (4%)	0	0	0	0	NS
Trisomy 7	2% (6/318)	4 (5%)	1 (1%)	1 (2%)	0	0	0	NS

Although the table shows distribution of secondary changes in classified cases, the overall percentage was estimated on the total samples analyzed for each gene/abnormality,

including unclassified and undetermined cases. % rounded up if > 0.5 and down if ≤ 0.5; the deletion of *NF1* and *SUZ12* was considered as a unique event as they were lost together in cases with del(17)(q11.2); *NOTCH1/FBXW7* mutations are summed up together with the other *secondary changes*; in bold privileged association as well as inverse correlations are indicated.

*chi-square test.

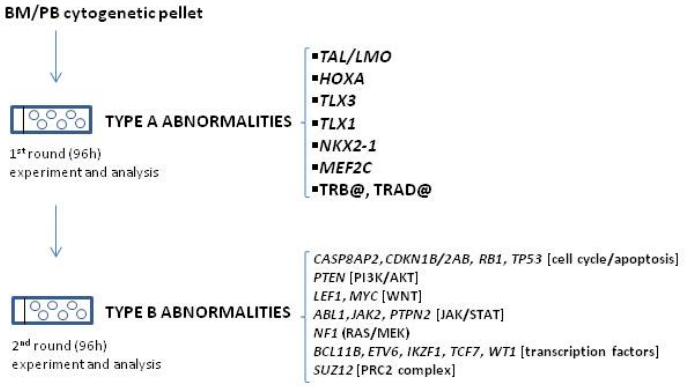
BM/PB cytogenetic pellet
TYPE A ABNORMALITIES
1st round (96h)
experiment and analysis
▪TAL/LMO
▪HOXA
▪TLX3
▪TLX1
▪NKX2-1
▪MEF2C
▪TRB@, TRAD@
TYPE B ABNORMALITIES
2nd round (96h)
experiment and analysis
CASP8AP2, CDKN1B/2AB, RB1, TP53 [cell cycle/apoptosis]
PTEN [PI3K/AKT]
LEF1, MYC [WNT]
ABL1, JAK2, PTPN2 [JAK/STAT]
NF1 (RAS/MEK)
BCL11B, ETV6, IKZF1, TCF7, WT1 [transcription factors]
SUZ12 [PRC2 complex]

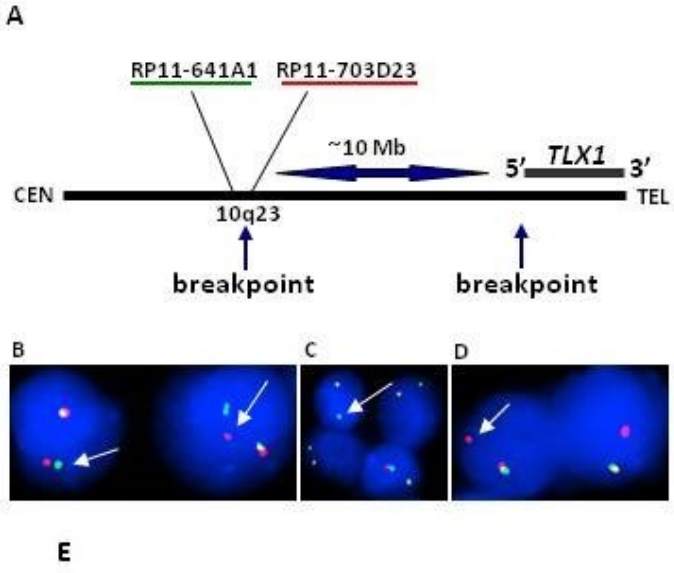
A
RP11-641A1
RP11-703D23
~10 Mb
5′ TLX1 3′
CEN
TEL
10q23
breakpoint
breakpoint
B
C
D

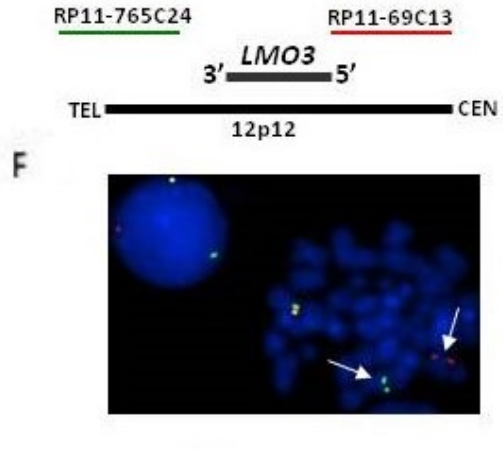
E
RP11-765C24
RP11-69C13
3′ LMO3 5′
TEL
CEN
12p12
F
TAL/LMO
HOXA
TLX3
TLX1
NKX2-1/2-2
MEF2C
UNCLASSIFIED
ETP/near-ETP

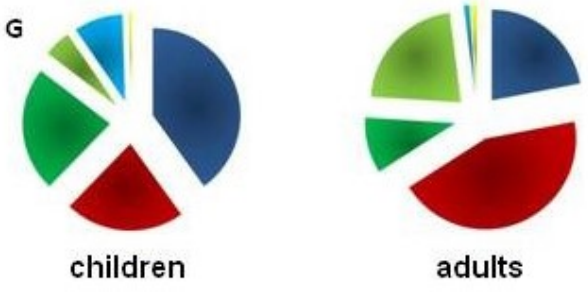
G
children
adults

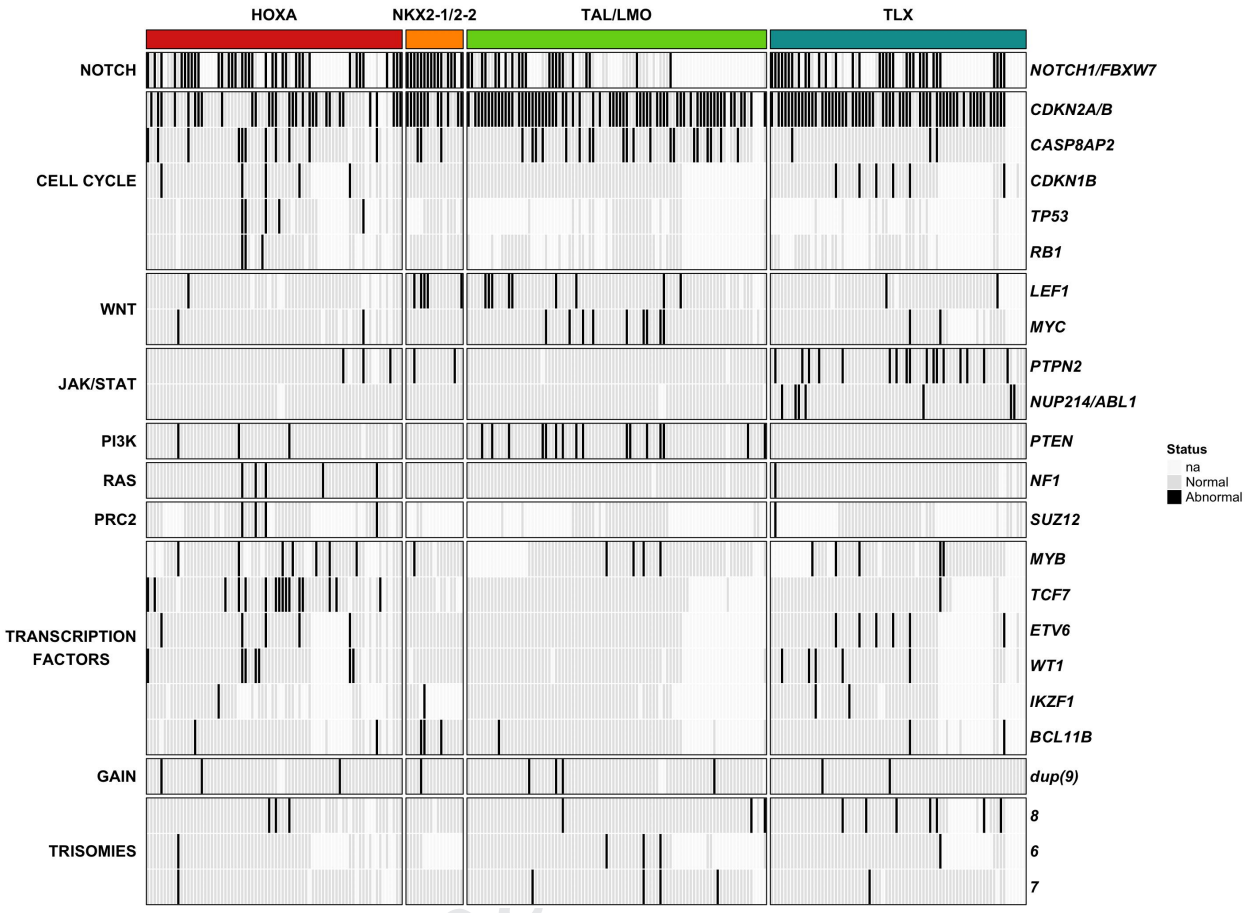
HOXA
NKX2-1/2-2
TAL/LMO
TLX
NOTCH
NOTCH1/FBXW7
CELL CYCLE
CDKN2A/B
CASP8AP2
CDKN1B
TP53
RB1
WNT
LEF1
MYC
JAK/STAT
PTPN2
NUP214/ABL1
PI3K
PTEN
RAS
NF1
PRC2
SUZ12
TRANSCRIPTION FACTORS
MYB
TCF7
ETV6
WT1
IKZF1
BCL11B
GAIN
dup(9)
TRISOMIES
8
6
7
Status
na
Normal
Abnormal

Supplemental Figure Legends

Supplemental Figure S1. Dual color fluorescence *in situ* hybridization (FISH) experiment with clones RP11-249M6+RP11-418C1/*MLLT10* (red) and RP1-167F23+RP5-1103I5/*HOXA* (green) in case UPN PGTALL30: the presence of three red and three green signals indicates that *HOXA* and *MLLT10* are both rearranged in the same cell.

Supplemental Figure S2. Shallow whole-genome sequencing (sWGS) data obtained from two primary T-ALL patient samples, ie. PGTALL275 (above; sWGS code 24016) and PGTALL215 (bottom; sWGS code 10241). Data have been processed, analyzed, and visualized by ViVar[30] and depicts copy number profiles from a region on the long arm of chromosome 10 ranging from 82 Mb to 134 Mb (regions marked by red rectangle). Each dot represents the normalized intensity of a specific genomic region of interest. Black dots correspond to genomic regions that are considered copy neutral, whereas red dots correspond to areas that are deleted at a statistically significant level. sWGS data obtained from two primary T-ALL patient samples, ie, PGTALL275 (above; sWGS code 24016) and PGTALL215 (bottom; sWGS code 10241). Copy number profiles are depicted from a region at 10q23 showing genomic deletions (red dots) near the TLX1 locus in both leukemic patient samples analyzed. Black dots correspond to regions without copy number changes.